

# Two-loop amplitude for mixed QCD-EW corrections to $gg \rightarrow Hg$

---

**Matteo Becchetti,<sup>a</sup> Francesco Moriello,<sup>b</sup> Armin Schweitzer<sup>b</sup>**

<sup>a</sup>*Dipartimento di Fisica, Università di Torino and INFN Sezione di Torino, Via Pietro Giuria 1, I-10125 Torino, Italy*

<sup>b</sup>*ETH Zürich, Institut für theoretische Physik, Wolfgang-Pauli Str. 27, 8093 Zürich, Switzerland*  
*E-mail: [matteo.becchetti@unito.it](mailto:matteo.becchetti@unito.it), [fmoriell@itp.phys.ethz.ch](mailto:fmoriell@itp.phys.ethz.ch), [armin.schweitzer@phys.ethz.ch](mailto:armin.schweitzer@phys.ethz.ch)*

**ABSTRACT:** We report on the two-loop amplitude computation for the mixed QCD-electroweak corrections to the process  $gg \rightarrow Hg$ , with exact dependence on the electroweak boson masses. This amplitude has been employed in the computation of next-to-leading order (NLO) mixed QCD-electroweak corrections to the Higgs-boson production rate in [1]. The master integrals that appear in the amplitude are evaluated by means of generalized power series expansions, which allows for fast and high-precision numerical evaluation of the amplitude in the physical phase-space, proving to be a powerful tool for phenomenological applications.

**KEYWORDS:** Higgs, QCD, Electroweak

---

## Contents

<b>1</b>	<b>Introduction</b>	<b>1</b>
<b>2</b>	<b>Overview of the computation</b>	<b>4</b>
<b>3</b>	<b>Computation of the amplitude</b>	<b>5</b>
3.1	Coupling structure of the light-quark contribution	6
3.2	Gauge invariant tensor decomposition	7
3.3	Functional relations	11
3.4	Validation of the amplitude	13
<b>4</b>	<b>Computation of the Master Integrals</b>	<b>13</b>
4.1	Differential equations approach	15
4.2	Series expansion method	16
4.3	Analytic continuation	18
4.4	Boundary conditions	19
<b>5</b>	<b>Conclusions</b>	<b>20</b>
<b>6</b>	<b>Acknowledgements</b>	<b>20</b>
<b>A</b>	<b>Example usage of the dedicated MadGraph5_aMC@NLO-plugin</b>	<b>21</b>

---

## 1 Introduction

The discovery of the Higgs boson [2, 3] concluded the long ongoing experimental search for the elementary particles described and predicted within the Standard Model (SM) of particle physics. This discovery can be seen as the starting point of a precision physics program which aims at the accurate determination of the model parameters and the rigorous assessment of the goodness of the theoretical predictions.

Part of this precision program has been focused on studying the Higgs sector, with one important aspect being the Higgs boson production via gluon fusion at the Large Hadron Collider (LHC) at CERN. Gluon fusion is by far the dominant Higgs production mode and it is thus of utmost importance to have a very accurate theoretical prediction of this process.

The coupling of the Higgs boson to gluons is mediated by a heavy-quark loop. The Higgs production cross section in gluon fusion was computed at leading order in the '70s [4],

and at next-to-leading-order (NLO) in the strong coupling constant  $\alpha_s$  in the '90s [5, 6]. The NLO QCD corrections are sizable ( $\sim +100\%$ ), therefore it is crucial to compute higher-order terms in the perturbative expansion to improve the accuracy of the predictions.

The next-to-next-to-leading-order (NNLO) [7–9] and the next-next-to-next-to-leading-order (N<sup>3</sup>LO) [10–15] corrections in  $\alpha_s$  have been computed in the Higgs Effective Field Theory (HEFT) approach, i.e. in the limit of a top quark much heavier than the Higgs boson,  $M_T \gg M_H$ . In this limit the loop-mediated coupling is replaced by an effective tree-level one. The NNLO corrections were found to be significant ( $\sim 10 - 20\%$ ) and with a reduced scale-dependent uncertainty. The N<sup>3</sup>LO corrections turn out to be small ( $\sim 4 - 6\%$ ) [16], with a renormalization/factorization scale variation of less than 2%.

Given the very high theoretical accuracy of the N<sup>3</sup>LO corrections, sub-dominant effects to the Higgs cross section, which are estimated to be in the percent range, have to be considered.

One kind of sub-dominant contribution to the cross section is given by the quark-mass effects. Firstly, the infinite top mass approximation has a  $\sim 6\%$  effect on the SM cross section with 5 massless flavors and the top. This effect is estimated from the NLO [17] prediction, and it can be improved through a multiplicative correction factor applied to the state-of-the-art N<sup>3</sup>LO HEFT computation. The finite top-mass contributions mostly factorize from the perturbative corrections [16], so that rescaling results in an estimated  $\sim 1\%$  uncertainty on the prediction [18, 19] only. However, this represents a sizeable portion of the remaining theoretical error. At NNLO, top-quark mass effects have been estimated through a power expansion in  $M_H/M_T$  [18, 20, 21] to be a  $\sim 1\%$  effect. Moreover, very recently [22] the NNLO-accurate prediction retaining the full top-mass dependence has been performed, thus effectively removing the residual uncertainty associated with non-factorizing top-mass effects.

A different kind of quark-mass effect is given by the contribution stemming from light-quarks. At NLO-accuracy, these finite light-quark mass-effects are known exactly [6, 17, 23–28] and contribute a  $\sim -7\%$  change [26] to the cross section, mainly due to top-bottom interferences. Although almost all<sup>1</sup> the relevant ingredients - double-virtual [29–31], real-virtual [32–34] and double-real [35, 36] - of the computation including all finite quark-mass effects at NNLO are available, such a computation has not been performed yet, resulting in a remaining residual uncertainty of  $\sim 0.8\%$ .

Beyond the quark-mass effects, another class of suppressed contribution to the Higgs cross section are the so-called “mixed QCD-electroweak (EW) effects”. They arise at two loops, i.e. at  $\mathcal{O}(\alpha^2\alpha_s^2)$ <sup>2</sup>, and are heavily suppressed due to the coupling hierarchy ( $\alpha \sim 10^{-1}\alpha_s$ ). They are due to the gluons coupling to EW bosons  $V = W, Z$  through a quark loop, followed by the gauge coupling of the EW bosons to the Higgs boson. Mixed QCD-EW

---

<sup>1</sup>The double-virtual corrections with both quark masses is not known yet.

<sup>2</sup>We count all factorized coupling constants except the strong coupling as  $\alpha$ .

contributions were calculated for the light-quark loop [37–39], for the heavy-quark loop [40] and with full quark-mass dependence [40], and found to increase the N<sup>3</sup>LO cross section by about 2% [16]. Since this increase is of the order of the residual QCD uncertainty, it is important to compute the NLO corrections in  $\alpha_s$ . They consist of three parts: the one-loop  $2 \rightarrow 3$ , the two-loop  $2 \rightarrow 2$ , and the three-loop  $2 \rightarrow 1$  with sample diagrams of the last two shown in the first column of table 1. In [41], the one-loop  $2 \rightarrow 3$  processes were computed and found to yield a negligible contribution. At LO ( $\sim \mathcal{O}(\alpha^2\alpha_s^2)$ ), the largest part ( $\sim 98\%$  [39]) of the mixed QCD-EW contributions is due to the light-quark part. The evaluation of the NLO ( $\sim \mathcal{O}(\alpha^2\alpha_s^3)$ ) corrections has, therefore, been aimed at the light-quark part only. These corrections were first estimated in the limit where the Higgs mass is much smaller than the EW boson masses,  $M_H \ll M_V$  [42] and they turned out to be sizable. The three-loop contribution was evaluated analytically and expressed in terms of multiple polylogarithms (MPLs) [43]. In [44], the soft part of the two-loop  $2 \rightarrow 2$  process was added, and in [45] the total cross section was evaluated in the small EW-boson mass limit,  $M_V \ll M_H$ . These different approximations gave consistent results. However, they do not allow for a detailed assessment of the remaining uncertainties, since boson-mass and hard effects could not be accessed precisely. Thus, the remaining uncertainty due to mixed QCD-EW contributions to the N<sup>3</sup>LO-accurate Higgs production cross section in gluon fusion remained a sizeable  $\pm 1\%$  [16]. This motivates the exact computation of mixed QCD-EW contributions at NLO.

The planar master integrals (MIs) for the two-loop  $gg \rightarrow Hg$  process with the exact EW-boson mass were published in [46] and in [47] the complete helicity amplitudes, including the non-planar diagrams, were presented. The calculation was done analytically, expressing the results in terms of MPLs.

In [1], we computed the NLO-accurate corrections to the mixed QCD-electroweak contributions to the Higgs-boson production rate. This computation removed the major uncertainty, i.e. the unknown exact hard-effects at NLO, and allowed for a significant reduction (almost a factor of two) of the uncertainty associated with mixed QCD-EW contributions to the gluon fusion Higgs production cross section at N<sup>3</sup>LO.

In this work we augment [1] by providing additional details on the computation of the two-loop amplitude for the partonic process  $gg \rightarrow Hg$ , with the exact EW-boson mass, used in the cross section computation, where we employed the generalized power series expansion method [48] to evaluate the master integrals appearing in the amplitude numerically. This method allows for fast and reliable numerical evaluation of the amplitude in the physical phase-space, proving to be a powerful tool for phenomenological applications [1]. Our result has been checked against ref. [47] and we found full agreement. We also provide ancillary material for the numerical evaluation of the MIs, and of the amplitude. While we exploited a private implementation of the generalized power series expansion method, the ancillary material can also be used within the software DIFFEXP [49] in order to obtain numerical

values for the MIs, and thus for the amplitude.

The paper is organized as follows. In section 2 we summarize the main results of the paper and we describe the general setup of the computation. In section 3 we describe in detail the amplitude computation, in particular we discuss the form factors decomposition and consistency checks that have been made to ensure the correctness of the calculation. Finally, in section 4 we present a brief review of the generalized power series method used to solve the system of differential equations associated to the (MIs) that appear in the amplitude.

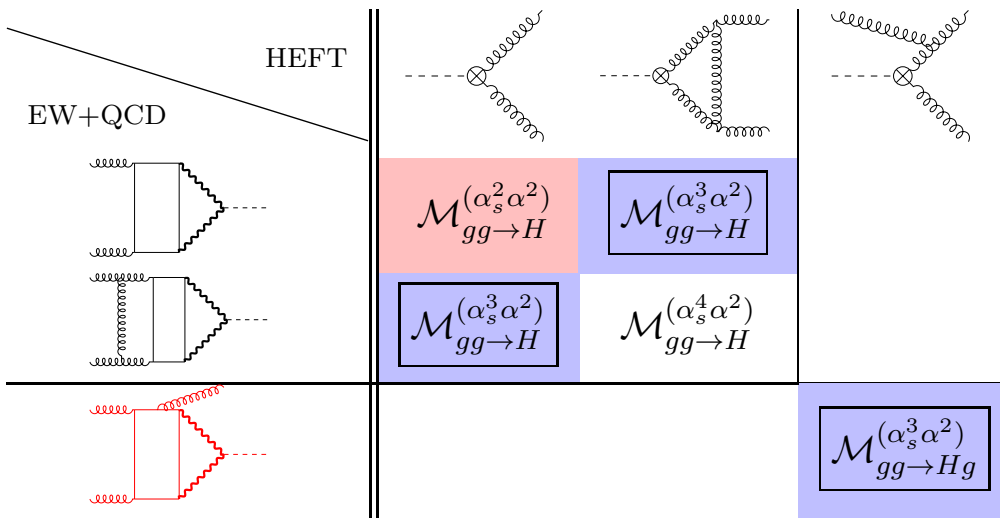


**Table 1:** Overview of the relevant interferences necessary for the computation of the cross sections  $\sigma_{gg \rightarrow H+X}^{(\alpha_s^2 \alpha^2 + \alpha_s^3 \alpha^2)}$  presented in [1]. The red colored cell is the LO and cells highlighted in blue are part of the NLO contribution. Amplitudes are denoted by a single representative diagram. Curly lines denote gluons, wavy lines massive weak gauge bosons, continuous straight lines massless quarks and the dashed line represents the Higgs boson. The red diagram at the bottom left is a representative for the two-loop amplitude considered in this work. Diagrams are drawn with TikZ-Feynman [50].

## 2 Overview of the computation

The main result of this paper is the computation of the two-loop amplitude for the partonic process  $g(p_1)g(p_2) \rightarrow g(p_3)H(p_4)$ . This is a necessary ingredient for the light-quark contribution to the NLO mixed QCD-electroweak (EW) corrections to Higgs production in gluon fusion at the LHC with exact dependence on the EW gauge boson masses [1].

The amplitude for the partonic process  $g(p_1)g(p_2) \rightarrow g(p_3)H(p_4)$  can be written as

$$\begin{aligned} \mathcal{A} = & -\frac{i}{2} f_{a_1 a_2 a_3} \left( -\frac{\sqrt{\alpha_{EW}^3 \alpha_s^3}}{4\pi s_w^3} m_W \right) \varepsilon_{\mu_1}(p_1, p_2) \varepsilon_{\mu_2}(p_2, p_1) \varepsilon_{\mu_3}^*(p_3, p_1) \\ & \times \sum_{i=1}^4 T_i^{\mu_1 \mu_2 \mu_3} \left( \sum_{V=W,Z} \frac{\kappa_V}{m_V^4} A_i \left( \frac{s}{m_V^2}, \frac{t}{m_V^2}, \frac{m_H^2}{m_V^2} \right) \right) \end{aligned} \quad (2.1)$$

with  $p_1^2 = p_2^2 = p_3^2 = 0$ ,  $p_4^2 = m_H^2$ ,  $s = (p_1 + p_2)^2$ ,  $t = (p_1 - p_3)^2$ ,  $m_H$  ( $m_V$ ) is the Higgs (weak) boson mass,  $\varepsilon(p_k, q_k)$  are polarization vectors for the external gluon  $k$  with reference momentum  $q_k$ , and the  $T_i$  are gauge-invariant Lorentz tensors derived in section 3.2. The global couplings due to light-quark contributions (see section 3.1) are

$$\kappa_W = 1, \quad \kappa_Z = \frac{1}{c_W^4} \left( \frac{11s_W^4}{9} - \frac{7s_W^2}{6} + \frac{5}{8} \right), \quad (2.2)$$

where  $\alpha_s$  ( $\alpha_{EW}$ ) denotes the strong (weak) coupling constant and  $s_W$  ( $c_W$ ) the sine (cosine) of the Weinberg angle. The  $A_i \left( \frac{s}{m_V^2}, \frac{t}{m_V^2}, \frac{m_H^2}{m_V^2} \right)$  are functions of the rescaled kinematic invariants and of the master integrals (MIs) defined in section 3, which we provide in the ancillary material.

The other main result for this paper is the evaluation of the relevant MIs for the two-loop amplitude (2.1) by means of the generalized power series expansion method [48]. The starting data for this method are the knowledge of the system of differential equations and a set of boundary points for the MIs; then the generalized series technique allows us to transport the boundary values to a new kinematic point. This method allows for fast high-precision numerical evaluation which can be improved by having a precomputed grid of boundary points. Moreover, the analytic continuation of the generalized series expansion in the physical region is completely algorithmic.

### 3 Computation of the amplitude

In this section we describe the details of the amplitude computation for the process under consideration. To obtain the amplitude we generate all relevant Feynman diagrams with QGraf [51], perform the color and Lorentz algebra with private computer codes and decompose it into a set of four gauge-invariant form factors. We then map all diagrams to a minimal set of two propagator structures and perform an Integration-by-Parts (IBP) reduction [52] to a minimal set of master integrals (MIs) with the computer code Kira [53, 54]. The MIs are computed as described in section 4. All computations are performed in conventional dimensional regularization (CDR) [55].

In the first section 3.1 we describe the decomposition of the amplitude into four form factors based on the coupling structure of the process, and we show that actually just one form factor,  $\mathcal{A}_{VV}$ , has to be explicitly computed. In section 3.2 we perform the tensor

decomposition of  $\mathcal{A}_{V\bar{V}}$ . Finally, in the third section 3.3, we discuss the derivation of functional relations exploited to simplify the amplitude, and in the last one, section 3.4, the checks performed to validate our result.

### 3.1 Coupling structure of the light-quark contribution

In the following we outline the coupling structure of the light-quark contribution eq. (2.1). In order to discuss the decomposition we separate the couplings of the quarks to the electroweak gauge bosons in SM as follows:

$$\begin{aligned} udW^+ &\propto g_{V,W}\gamma^\mu + g_{A,W}\gamma^\mu\gamma^5, \\ udW^- &\propto g_{V,W}^*\gamma^\mu + g_{A,W}^*\gamma^\mu\gamma^5, \\ qqZ &\propto g_{V,Z}\gamma^\mu + g_{A,Z}\gamma^\mu\gamma^5. \end{aligned} \quad (3.1)$$

We refer to  $g_V$  as the vector coupling constant, and to  $g_A$  as the axial coupling constant. Following this coupling separation we may write the mixed QCD-EW amplitude as:

$$\begin{aligned} \mathcal{A} &= \mathcal{A}_{V\bar{V}} + \mathcal{A}_{A\bar{V}} + \mathcal{A}_{V\bar{A}} + \mathcal{A}_{A\bar{A}} \\ &= \sum_{vb=(ZZ,W^\pm W^\mp)} g_{H,vb} (g_{V,vb}^2 A_{V\bar{V}} + g_{A,vb} g_{V,vb} A_{A\bar{V}} + g_{V,vb} g_{A,vb} A_{V\bar{A}} + g_{A,vb}^2 A_{A\bar{A}}), \end{aligned} \quad (3.2)$$

where  $g_{H,vb}$  is the coupling of the weak bosons to the Higgs. This decomposition highlights the coupling structure of the electroweak loop with representative diagrams shown in the first column of table 1. In order to compute the mixed QCD-EW cross section, we are interested in the interference of electroweak amplitudes against the pure QCD background shown in the first row of table 1. Therefore, for the cross section under consideration, the mixed coupling structures  $A_{V\bar{A}}$  and  $A_{A\bar{V}}$  are of no concern, since they will not contribute to the interferences. In particular, the relevant amplitude can thus be written as:

$$\mathcal{A} = \mathcal{A}_{V\bar{V}} + \mathcal{A}_{A\bar{A}} = \sum_{vb=(ZZ,W^\pm W^\mp)} g_{H,vb} (g_{V,vb}^2 A_{V\bar{V}} + g_{A,vb}^2 A_{A\bar{A}}). \quad (3.3)$$

This also implies that the subtleties arising in the embedding of  $\gamma^5$  into CDR do not arise in our computation, since the  $\gamma^5$ -odd traces do not contribute<sup>3</sup>. We can treat  $\gamma^5$  as completely anti-commuting and one can show that the pure vector-piece  $A_{V\bar{V}}$  and the pure axial-piece  $A_{A\bar{A}}$  are equal:

$$A_{V\bar{V}} = A_{A\bar{A}}. \quad (3.4)$$

This is due to the fact that all the relevant  $\gamma$ -chains of  $A_{A\bar{A}}$  are of the form:

$$\gamma^5 \gamma^{\mu_1} \dots \gamma^{\mu_{2n}} \gamma^5 = \gamma^{\mu_1} \dots \gamma^{\mu_{2n}}, \quad (3.5)$$

---

<sup>3</sup>They appear in the neglected  $A_{V\bar{A}(A\bar{V})}$ -pieces only

where  $n$  is an integer.

The second simplification of the amplitude computation arises solely from phenomenological considerations. As already alluded to in the introduction, the top-quark contribution to the mixed QCD-EW cross section at LO makes up only  $\sim 2\%$  of the contribution. It is reasonable to expect a similar behaviour at NLO and we therefore restrict ourselves to the computation of the light-quark contributions, e.g. 5 massless flavors. Removing the top-quark will manifestly break gauge invariance, since the  $SU(2)$ -doublet involving the left-handed top is effectively removed from the computation. We implement it in practical terms by restricting the  $W$ -exchange contribution to a diagonal mixing matrix where we neglect the top-bottom flavour exchange, such that:

$$g_{A,W^\pm W^\mp}^2 = g_{V,W^\pm W^\mp}^2 = -\frac{1}{4} \frac{g^2}{2} \sum_{\{(u,d),(c,s)\}} 1 = -\frac{1}{4} g^2, \quad (3.6)$$

while for the  $Z$ -boson exchange we include the bottom quark and obtain

$$\begin{aligned} g_{A,ZZ}^2 &= -\frac{1}{4} \frac{g^2}{c_W^2} \sum_{f=\{u,c,d,s,b\}} (T_f^3)^2 = -\frac{5}{16c_W} g^2, \\ g_{V,ZZ}^2 &= -\frac{1}{4} \frac{g^2}{c_W^2} \sum_{f=\{u,c,d,s,b\}} (T_f^3 - 2Q_f s_w^2)^2 = -\frac{(176s_w^4 - 168s_w^2 + 45)}{144c_W^2} g^2, \end{aligned} \quad (3.7)$$

where  $s_W$  ( $c_W$ ) denotes the sine (cosine) of the Weinberg mixing angle,  $T_f^3$  the weak isospin, and  $Q_f$  the electric charge.

Following the previous discussion, when we compute mixed amplitudes, we are concerned with the computation of the pure vector piece  $A_{VV}$  for an arbitrary vector boson with mass  $m_V$  and a massless quark. The  $A_{AA}$  pieces, the relevant quark flavours, and the  $W$ - and  $Z$ -bosons are then restored by inserting the associated couplings in eq. (3.3):

$$\begin{aligned} \mathcal{A} &= \sum_{vb=(ZZ,W^\pm W^\mp)} g_{H,vb} (g_{V,vb}^2 A_{VV} + g_{A,vb}^2 A_{AA}) \\ &= g_{H,ZZ} (g_{V,ZZ}^2 + g_{A,ZZ}^2) A_{VV}(m_Z) + 2g_{H,WW} (g_{V,WW}^2 + g_{A,WW}^2) A_{VV}(m_W) \\ &= -g^3 m_W \left( \frac{1}{c_W^4} \left( \frac{11s_w^4}{9} - \frac{7s_w^2}{6} + \frac{5}{8} \right) A_{VV}(m_Z) + A_{VV}(m_W) \right), \end{aligned} \quad (3.8)$$

where the factor two accounts for the  $W^+W^-$  and  $W^-W^+$  configuration and  $\alpha_{EW} = \frac{g^2 s_w^2}{4\pi}$ . Including the color-factors we arrive at the coupling structure in eq. (2.1).

### 3.2 Gauge invariant tensor decomposition

In order to perform the analytic computation one is interested in decomposing the amplitude into a minimal set of gauge-invariant tensor structures defined by the external particles of the process under consideration. Such a tensor decomposition involves the analytic solution of potentially large systems. Here, the large size of these systems is mainly



due to the regularization scheme choice. When we work in CDR, we lift all structures to  $d$ -dimensions. Such a treatment has many advantages, e.g. renormalization constants are particularly easy, and one does not have to treat external structures differently from off-shell structures. However, it also comes with drawbacks, e.g. one can not easily define explicit helicity states, and the lift of the Dirac-structures becomes non-trivial since one does not have a finite basis as for the four-dimensional case. In comparison, for example, the 't Hooft-Veltman scheme keeps the external structure, e.g. external momenta, polarizations, and spinors, in strictly four dimensions. It explicitly splits the algebra and the loop-momenta into 4-dimensional, and  $-2\varepsilon$ -dimensional orthogonal components, and requires introducing additional renormalization pieces, which account for this splitting. However, keeping the external states strictly four-dimensional has advantages. In particular, one can work with physical, on-shell amplitudes, e.g. defined helicity states, which gets rid of unphysical, spurious structures. Such an approach can simplify the construction of the projectors by not projecting on generic, Ward-identity fulfilling Lorentz structures, but specific helicity states. This was put forward in a general approach recently in [56, 57] and [58], and we refer to the discussion and references therein for more details.

In our computation we do not work within the framework of helicity amplitudes. Instead we follow the more “traditional” multi-loop approach, in which a set of projectors for generic helicities is obtained, see e.g. [59–61], that can be applied to project the amplitude onto a minimal set of Ward-identity fulfilling, independent tensor structures. The derivation of the decomposition for the amplitude under consideration is detailed in the following.

The amplitude for the vector piece of the process  $g(p_1) g(p_2) \rightarrow g(p_3) H(p_4)$  may be written as:

$$A_{\text{VV}} = \sum_{i=1}^{14} t_i S_i \quad (3.9)$$

where the  $t_i$  are all possible rank-three Lorentz-tensors obtained from the metric and the external momenta, and the  $S_i$  are scalar loop-integrals independent of the polarization vectors. The tensor-structures are:

$$p_{i \neq 1}^{\mu_1} p_{j \neq 2}^{\mu_2} p_{k \neq 3}^{\mu_3} |_{i \neq j \neq k \neq i} : \quad t_1 = (\varepsilon_1 p_2)(\varepsilon_2 p_3)(\varepsilon_3^* p_1) \quad t_2 = (\varepsilon_1 p_3)(\varepsilon_2 p_1)(\varepsilon_3^* p_2) \quad (3.10)$$

$$p_{i \neq 1}^{\mu_1} p_1^{\mu_2} p_1^{\mu_3} : \quad t_3 = (\varepsilon_1 p_2)(\varepsilon_2 p_1)(\varepsilon_3^* p_1) \quad t_4 = (\varepsilon_1 p_3)(\varepsilon_2 p_1)(\varepsilon_3^* p_1) \quad (3.11)$$

$$p_2^{\mu_1} p_{i \neq 2}^{\mu_2} p_2^{\mu_3} : \quad t_5 = (\varepsilon_1 p_2)(\varepsilon_2 p_1)(\varepsilon_3^* p_2) \quad t_6 = (\varepsilon_1 p_2)(\varepsilon_2 p_3)(\varepsilon_3^* p_2) \quad (3.12)$$

$$p_3^{\mu_1} p_3^{\mu_2} p_{i \neq 3}^{\mu_3} : \quad t_7 = (\varepsilon_1 p_3)(\varepsilon_2 p_3)(\varepsilon_3^* p_1) \quad t_8 = (\varepsilon_1 p_3)(\varepsilon_2 p_3)(\varepsilon_3^* p_2) \quad (3.13)$$

$$g^{\mu_1 \mu_2} p_{i \neq 3}^{\mu_3} : \quad t_9 = (\varepsilon_1 \varepsilon_2)(\varepsilon_3^* p_1) \quad t_{10} = (\varepsilon_1 \varepsilon_2)(\varepsilon_3^* p_2) \quad (3.14)$$

$$g^{\mu_1 \mu_3} p_{i \neq 2}^{\mu_2} : \quad t_{11} = (\varepsilon_1 \varepsilon_3^*)(\varepsilon_2 p_1) \quad t_{12} = (\varepsilon_1 \varepsilon_3^*)(\varepsilon_2 p_3) \quad (3.15)$$

$$g^{\mu_2 \mu_3} p_{i \neq 1}^{\mu_1} : \quad t_{13} = (\varepsilon_2 \varepsilon_3^*)(\varepsilon_1 p_2) \quad t_{14} = (\varepsilon_2 \varepsilon_3^*)(\varepsilon_1 p_3) \quad (3.16)$$

where the first element of each line states the Lorentz-structure that gives rise to the  $t_i$  and transversality of the polarizations ( $p_i \varepsilon_i = 0$ ) is imposed.

Requiring gauge invariance,

$$A_{VV}|_{\varepsilon(p_i) \rightarrow p_i} = 0, \quad i = 1, \dots, 3, \quad (3.17)$$

one finds relations between the  $S_i$ , and the amplitude may be written as

$$\begin{aligned} A_{VV} &= \sum_{i=1}^4 T_i A_i \\ &= \sum_{i=1}^4 (\varepsilon_{\mu_1}(p_1) \varepsilon_{\mu_2}(p_2) \varepsilon_{\mu_3}^*(p_3) T_i^{\mu_1 \mu_2 \mu_3}) A_i, \end{aligned} \quad (3.18)$$

where the  $A_i$  are linear combinations of the  $S_i$  in eq. (3.9). The  $T_i$  fulfill Ward identities independently. Their components are

$$T_1^{\mu_1 \mu_2 \mu_3} = -\frac{(s_{23} p_1^{\mu_3} - s_{13} p_2^{\mu_3})(s_{12} g^{\mu_1 \mu_2} - 2p_2^{\mu_1} p_1^{\mu_2})}{2s_{23}}, \quad (3.19)$$

$$T_2^{\mu_1 \mu_2 \mu_3} = -\frac{(s_{13} p_2^{\mu_1} - s_{12} p_3^{\mu_1})(s_{23} g^{\mu_2 \mu_3} - 2p_3^{\mu_2} p_2^{\mu_3})}{2s_{13}}, \quad (3.20)$$

$$T_3^{\mu_1 \mu_2 \mu_3} = -\frac{(s_{23} p_1^{\mu_2} - s_{12} p_3^{\mu_2})(s_{13} g^{\mu_1 \mu_3} - 2p_3^{\mu_1} p_1^{\mu_3})}{2s_{23}}, \quad (3.21)$$

$$\begin{aligned} T_4^{\mu_1 \mu_2 \mu_3} &= \frac{1}{2} (g^{\mu_2 \mu_3} (s_{13} p_2^{\mu_1} - s_{12} p_3^{\mu_1}) + g^{\mu_1 \mu_3} (s_{12} p_3^{\mu_2} - s_{23} p_1^{\mu_2}) \\ &\quad + g^{\mu_1 \mu_2} (s_{23} p_1^{\mu_3} - s_{13} p_2^{\mu_3}) - 2(p_2^{\mu_1} p_3^{\mu_2} p_1^{\mu_3} - p_3^{\mu_1} p_1^{\mu_2} p_2^{\mu_3})), \end{aligned} \quad (3.22)$$

with  $s_{ij} = 2(p_i p_j)$ .

These tensor-structures are not unique. In order to see this, consider  $A_{VV}|_{\varepsilon_1 \rightarrow p_1} = 0$  from eq. (3.9):

$$\begin{aligned} A|_{\varepsilon_1 \rightarrow p_1} &= 0 \quad (3.23) \\ \Rightarrow 0 &= [S_6(p_1 p_2) + S_8(p_1 p_3)] (\varepsilon_2 p_3) (\varepsilon_3^* p_2) \\ &\quad + [S_2(p_1 p_3) + S_5(p_1 p_2) + S_{10}] (\varepsilon_2 p_1) (\varepsilon_3^* p_2) \\ &\quad + [S_3(p_1 p_2) + S_4(p_1 p_3) + S_9 + S_{11}] (\varepsilon_2 p_1) (\varepsilon_3^* p_1) \\ &\quad + [S_1(p_1 p_2) + S_7(p_1 p_3) + S_{12}] (\varepsilon_2 p_3) (\varepsilon_3^* p_1) \\ &\quad + [S_{13}(p_1 p_2) + S_{14}(p_1 p_3)] (\varepsilon_2 \varepsilon_3^*). \end{aligned} \quad (3.24)$$

Here, each term in the square-brackets, multiplying the contracted polarization, has to vanish resulting in five relations among linear combinations of the  $S_i$ . Once we impose the other Ward identities as well, we get a total of 15 equations (5 from each Ward-identity). Some of the relations will be linear combinations of others and in order to solve the overdetermined system efficiently, we introduce a strict ordering  $S_i \prec S_j$  if  $i < j$  and solve w.r.t. the variable with the highest ordering. This is in complete analogy to the well

known Laporta-algorithm used in the integration-by-parts (IBP) reduction to scalar MIs. For example, from the first Ward-identity above we get, using this particular ordering:

$$S_8 = -\frac{S_6(p_1 p_2)}{(p_1 p_3)}, \quad S_{10} = -S_2(p_1 p_3) - S_5(p_1 p_2), \quad (3.25)$$

$$S_{11} = -S_3(p_1 p_2) - S_4(p_1 p_3) - S_9, \quad S_{12} = -S_1(p_1 p_2) - S_7(p_1 p_3), \quad (3.26)$$

$$S_{14} = -\frac{S_{13}(p_1 p_2)}{(p_1 p_3)}. \quad (3.27)$$

As for the IBP-reduction, the choice of the ordering will define a different set of independent  $S_i$  (similar to the case of MIs), which will ultimately result in different gauge invariant Lorentz-tensors  $T_i$ . In particular, some ordering choices may give a “better” (e.g. more compact) definition of the basis of tensor structures than others.

To extract the scalar components  $A_i$  from the amplitude  $A_{\text{VV}}$  (see eq. (3.18)), one can construct “projectors”, denoted as  $P_i$  such that

$$\begin{aligned} \langle P_i, T_j \rangle &:= \sum_{\text{hel.}} (\varepsilon_{\nu_1}^*(p_1) \varepsilon_{\nu_2}^*(p_2) \varepsilon_{\nu_3}(p_3) P_i^{\nu_1 \nu_2 \nu_3}) \left( \varepsilon_{\mu_1}(p_1) \varepsilon_{\mu_2}(p_2) \varepsilon_{\mu_3}^*(p_3) T_j^{\mu_1 \mu_2 \mu_3} \right) \\ &= \delta_{ij}. \end{aligned} \quad (3.28)$$

In particular, if the  $T_i$  are a complete set of linearly independent Lorentz structures for the process under consideration, the projectors may be decomposed as

$$P_k = \sum_{i=1}^4 c_{k,i} T_i, \quad (3.29)$$

where the  $c_{k,i}$  are rational functions of the Mandelstam variables and the dimension. Denoting the reference vector for the external momentum  $p_i$  as  $q_i$  one can consider

$$\begin{aligned} \langle P_i, T_j \rangle &= \sum_{\text{hel.}} (\varepsilon_{\nu_1}^*(p_1) \varepsilon_{\nu_2}^*(p_2) \varepsilon_{\nu_3}(p_3) P_i^{\nu_1 \nu_2 \nu_3}) \left( \varepsilon_{\mu_1}(p_1) \varepsilon_{\mu_2}(p_2) \varepsilon_{\mu_3}^*(p_3) T_j^{\mu_1 \mu_2 \mu_3} \right) \\ &= \sum_{k=1}^4 c_{i,k} T_k^{\nu_1 \nu_2 \nu_3} \left( -g_{\mu_1 \nu_1} + \frac{(p_1)_{\mu_1} (q_1)_{\nu_1} + (q_1)_{\mu_1} (p_1)_{\nu_1}}{(p_1 q_1)} \right) \\ &\quad \left( -g_{\mu_2 \nu_2} + \frac{(p_2)_{\mu_2} (q_2)_{\nu_2} + (q_2)_{\mu_2} (p_2)_{\nu_2}}{(p_2 q_2)} \right) \\ &\quad \left( -g_{\mu_3 \nu_3} + \frac{(p_3)_{\mu_3} (q_3)_{\nu_3} + (q_3)_{\mu_3} (p_3)_{\nu_3}}{(p_3 q_3)} \right) T_j^{\mu_1 \mu_2 \mu_3} \\ &= \sum_{k=1}^4 c_{i,k} T_k^{\nu_1 \nu_2 \nu_3} (-g_{\mu_1 \nu_1}) (-g_{\mu_2 \nu_2}) (-g_{\mu_3 \nu_3}) T_j^{\mu_1 \mu_2 \mu_3}, \end{aligned} \quad (3.30)$$

where we used that by construction  $T|_{\varepsilon^*(p_i) \rightarrow p_i} = T|_{\varepsilon(p_i) \rightarrow p_i} = 0$ . Thus,  $\langle P_i, T_j \rangle$  is independent of the chosen reference momentum, and it is sufficient that

$$(P_{i, \mu_1 \mu_2 \mu_3} T_j^{\mu_1 \mu_2 \mu_3}) = -\delta_{ij}, \quad (3.31)$$

where the  $-1$  is a direct consequence of exchanging polarization sums of the inner product  $\langle \cdot, \cdot \rangle$  for Lorentz-contractions of the respective coefficients. The components of the “projectors”  $P_i$  can then be constructed as

$$P_i^{\mu_1\mu_2\mu_3} = -(B^{-1})_{ij} T_j^{\mu_1\mu_2\mu_3}, \quad (3.32)$$

where

$$B_{ij} = (T_{i,\mu_1\mu_2\mu_3} T_j^{\mu_1\mu_2\mu_3}), \quad (3.33)$$

since

$$P_i^{\mu_1\mu_2\mu_3} T_{j,\mu_1\mu_2\mu_3} = -(B^{-1})_{ik} T_k^{\mu_1\mu_2\mu_3} T_{j,\mu_1\mu_2\mu_3} = -(B^{-1})_{ik} B_{kj} = -\delta_{ij}. \quad (3.34)$$

For the tensor structures in (3.22) one finds, following this procedure, the components of the projectors:

$$\begin{aligned} -P_1^{\mu_1\mu_2\mu_3} &= -\frac{ds_{23}T_1^{\mu_1\mu_2\mu_3}}{(d-3)s_{12}^2s_{13}} - \frac{(d-4)T_2^{\mu_1\mu_2\mu_3}}{(d-3)s_{12}^2s_{23}} + \frac{(d-4)s_{23}T_3^{\mu_1\mu_2\mu_3}}{(d-3)s_{12}^2s_{13}^2} \\ &\quad - \frac{(d-2)T_4^{\mu_1\mu_2\mu_3}}{(d-3)s_{12}^2s_{13}}, \\ -P_2^{\mu_1\mu_2\mu_3} &= -\frac{(d-4)T_1^{\mu_1\mu_2\mu_3}}{(d-3)s_{12}^2s_{23}} - \frac{ds_{13}T_2^{\mu_1\mu_2\mu_3}}{(d-3)s_{12}s_{23}^3} + \frac{(d-4)T_3^{\mu_1\mu_2\mu_3}}{(d-3)s_{12}s_{13}s_{23}} \\ &\quad - \frac{(d-2)T_4^{\mu_1\mu_2\mu_3}}{(d-3)s_{12}s_{23}^2}, \\ -P_3^{\mu_1\mu_2\mu_3} &= \frac{(d-4)s_{23}T_1^{\mu_1\mu_2\mu_3}}{(d-3)s_{12}^2s_{13}^2} + \frac{(d-4)T_2^{\mu_1\mu_2\mu_3}}{(d-3)s_{12}s_{13}s_{23}} - \frac{ds_{23}T_3^{\mu_1\mu_2\mu_3}}{(d-3)s_{12}s_{13}^3} \\ &\quad + \frac{(d-2)T_4^{\mu_1\mu_2\mu_3}}{(d-3)s_{12}s_{13}^2}, \\ -P_4^{\mu_1\mu_2\mu_3} &= -\frac{(d-2)T_1^{\mu_1\mu_2\mu_3}}{(d-3)s_{12}^2s_{13}} - \frac{(d-2)T_2^{\mu_1\mu_2\mu_3}}{(d-3)s_{12}s_{23}^2} + \frac{(d-2)T_3^{\mu_1\mu_2\mu_3}}{(d-3)s_{12}s_{13}^2} \\ &\quad - \frac{dT_4^{\mu_1\mu_2\mu_3}}{(d-3)s_{12}s_{13}s_{23}}, \end{aligned} \quad (3.35)$$

where  $d = 4 - 2\varepsilon$ . In particular, for projecting the amplitude  $A_{\text{VV}}$  onto the  $T_i$ , we choose the reference momenta to be  $q_{1(2)} = p_{2(1)}$  and  $q_3 = p_1$ . The tensor-structures eq. (3.22) agree with the ones given in [61] under re-labeling, e.g. the same ordering for solving the overdetermined system in the determination of the independent  $T_i$  was used.

### 3.3 Functional relations

The amplitude  $A_{\text{VV}}$  is the leading-order amplitude for the partonic process  $gg \rightarrow Hg$  with the electroweak loop. Therefore, it is free of explicit poles in the dimensional regulator and only has implicit singularities in the IR-singular configurations. However, due to the IBP-reductions and the projections, the obtained result has spurious explicit poles multiplying

different Laurent coefficients of the canonical MIs  $f_i$ . The semi-analytic integration we employ (see section 4.2) does not give a result in terms of special functions and, therefore, functional relations are not explicit, e.g. we do not have manifest cancellations of spurious poles in the dimensional regulator. In the following, we outline how the explicit functional relations can be obtained by exploiting the fact that our set of MIs are canonical. This can directly be used to impose cancellation of spurious poles and it simplifies the amplitude considerably.

For this we consider the explicit (spurious) pole of order  $j$  of the scalar form-factor:

$$A^{(-j)} = \frac{1}{\varepsilon^j} \sum_k \sum_{i_k} \alpha_{j,k,i_k}(\vec{x}) f_{i_k}^{(k)} \quad (3.36)$$

where  $\alpha_{j,k,i_k}(\vec{x})$  is an algebraic function of the external scales and  $f_{i_k}^{(k)}$  is the  $k$ -th Laurent coefficient of the  $i_k$ -th canonical integral. In order for this pole to vanish, we first notice that the Laurent coefficients  $f_{i_k}^{(k)}$  are transcendental functions of weight  $k$ . This directly implies that there is a set of  $\mathbb{Q}$ -linear independent algebraic functions  $\alpha_{j,m,k}(\vec{x})$ , such that

$$A^{(-j)} = \frac{1}{\varepsilon^j} \sum_k \sum_m \alpha_{j,m,k}(\vec{x}) \left( \sum_{i_m} q_{i_m} f_{i_m}^{(k)} \right) \quad (3.37)$$

where  $q_{i_m} \in \mathbb{Q}$ , and

$$A^{(-j)} = 0 \quad \Rightarrow \quad F_m = \left( \sum_{i_m} q_{i_m} f_{i_m}^{(k)} \right) = 0, \quad \forall m. \quad (3.38)$$

$F_m$  is a functional relation between Laurent coefficients of weight  $k$ .

In order to obtain the functional relations  $F_m$  between the weight  $k$ -coefficients of the canonical MIs we proceed as follows. For each spurious pole of the amplitude  $A^{(-j)}$  we obtain the analytic coefficients  $\vec{\alpha}_{j,k}$  in front of all weight  $k$  integrals such that

$$A^{(-j)} = \frac{1}{\varepsilon^j} \sum_k \left( \vec{\alpha}_{j,k} \cdot \vec{f}^{(k)} \right), \quad (3.39)$$

where  $\cdot$  is the usual scalar product. We then build a matrix  $A_{\text{num.}}$  where each row is  $\vec{\alpha}_{j,k}$  evaluated at  $(s/m_V^2, t/m_V^2, m_H^2/m_V^2) = \vec{\pi} = (\pi_1, \pi_2, \pi_3)$  where the  $\pi_i$  are different and sufficiently large prime numbers. The sampling is performed for more (distinct) prime-tuples  $\vec{\pi}$  than there are weight  $k$  integrals in  $A^{(-j)}$ . The row-reduction  $A_{\text{num.}}^{\text{row-red.}}$  of  $A_{\text{num.}}$  will have  $n$  non-zero rows with elements  $q_{i_m} \in \mathbb{Q}$ , each corresponding to one of the functional relations eq. (3.38):

$$F_m = \left( \sum_{i_m} q_{i_m} f_{i_m}^{(k)} \right) = 0 \quad \Leftrightarrow \quad \exists l : \sum_{i_l} \left( A_{\text{num.}}^{\text{row-red.}} \right)_{l,i_l} f_{i_l}^{(k)} = F_m = 0. \quad (3.40)$$

We use this sampling to reveal 444 functional identities between Laurent coefficients of scalar integrals up to weight 3, effectively by-passing the analytic decomposition eq. (3.37).

This approach is very efficient, since row-reductions of large numeric matrices is not a bottleneck. We then impose these relations to make the vanishing of the spurious poles manifest, which, as a by-product, simplifies the finite remainder considerably.

### 3.4 Validation of the amplitude

In order to validate our result for the two-loop amplitude for  $gg \rightarrow Hg$  we performed a variety of checks.

First, we verified that our amplitude reproduces numerically the  $gg \rightarrow Hg$ -HEFT one in the limit  $m_V \rightarrow \infty$  as predicted by the infinite boson mass approximation [42].

Furthermore, we validated the interference of our amplitude against the interference obtained from the helicity amplitudes provided in [47]. This could only be done in the Euclidean regime, since in order to obtain the full set of helicity amplitudes from [47] one needs to relabel their results, which amounts to a kinematic crossing into a regime for which [47] does not provide the analytic continuation.

Lastly, in [1] we used our amplitude to compute the light quark-contribution of the NLO mixed QCD-electroweak contribution to the gluon fusion Higgs production cross section. In this computation, we perform our phase-space integration with two different local subtraction schemes (see [1] for more details), both of which are fully automatized, generic, and independent implementations. As a consequence errors occurring in the amplitude expression would have been seen as missed numerical cancellations in the IR, which do not occur. This is a powerful additional check since it happens independently at runtime and for physical kinematics.

## 4 Computation of the Master Integrals

In this section we discuss the computation of the MIs that appear in the amplitude  $\mathcal{A}$  eq. (2.1), which has been performed by means of the differential equation approach [62–64] together with the generalized series method [48] in order to obtain numerical results for MIs in the physical region. For the computation we heavily rely on the publicly available IBP-reduction programs Kira [53, 54, 65], Fire [66–69], and LiteRed [70, 71].

If one allows for the permutations:

$$\begin{aligned}
 \text{Map I: } & p_1 \rightarrow p_1 \quad p_2 \rightarrow -p_3 \quad p_3 \rightarrow -p_2, \\
 \text{Map II: } & p_1 \rightarrow p_2 \quad p_2 \rightarrow p_1 \quad p_3 \rightarrow p_3, \\
 \text{Map III: } & p_1 \rightarrow -p_3 \quad p_2 \rightarrow p_2 \quad p_3 \rightarrow -p_1,
 \end{aligned} \tag{4.1}$$

all the scalar integrals appearing in the  $A_i$  in eq. (3.18) can be considered as (sub-)topologies of the propagator sets shown in table 2.

The associated graphs, corresponding to the propagators  $D_{1,(P,NP)}, \dots, D_{7,(P,NP)}$  are depicted in fig. 1. Here, continuous lines denote massless propagators and wavy lines correspond to the massive gauge-boson propagators.

$P$	$NP$
$D_{1,P} = k_1^2$	$D_{1,NP} = k_1^2$
$D_{2,P} = (k_1 - k_2)^2$	$D_{2,NP} = (k_1 - k_2)^2$
$D_{3,P} = (k_1 + p_1)^2$	$D_{3,NP} = (k_1 + p_1)^2$
$D_{4,P} = (k_1 + p_1 + p_2)^2$	$D_{4,NP} = (k_1 + p_1 + p_2)^2$
$D_{5,P} = (-k_1 - p_3)^2$	$D_{5,NP} = (k_1 - k_2 - p_3)^2$
$D_{6,P} = (k_2 + p_1 + p_2)^2 - m_V^2$	$D_{6,NP} = (k_2 + p_1 + p_2)^2 - m_V^2$
$D_{7,P} = (-k_2 - p_3)^2 - m_V^2$	$D_{7,NP} = (-k_2 - p_3)^2 - m_V^2$
$D_{8,P} = (k_1 - k_2 - p_3)^2$	$D_{8,NP} = (-k_1 - p_3)^2$
$D_{9,P} = (k_2 + p_2)^2$	$D_{9,NP} = (k_2 + p_2)^2$

**Table 2:** Propagator sets for the scalar topologies in  $gg \rightarrow Hg$ . External momenta are denoted by  $p_i$  and loop-momenta by  $k_i$ , where  $p_i^2 = 0$ ,  $(p_1 + p_2 - p_3)^2 = m_H^2$ , and  $m_V$  denotes the gauge boson masses  $m_Z$  or  $m_W$ .

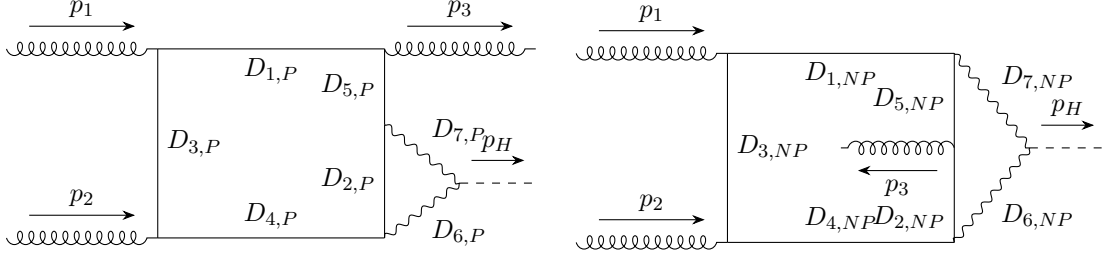


**Figure 1:** The scalar top-topologies associated to the propagator sets in table 2. Continuous lines denote massless propagators, wavy lines denote massive propagators. All external particles are on-shell.

The two-loop scalar integrals can be written in dimensional regularization as

$$\mathcal{J}_{a_1, \dots, a_9}^{(P, NP)} = \int \mathcal{D}^d k_1 \mathcal{D}^d k_2 \frac{D_{8,(P, NP)}^{a_8} D_{9,(P, NP)}^{a_9}}{D_{1,(P, NP)}^{a_1} \cdots D_{7,(P, NP)}^{a_7}}, \quad (4.2)$$

where  $a_i \geq 0$  are positive integers,  $d = 4 - 2\epsilon$  and the integration measure is defined as

$$\mathcal{D}^d k_i = \frac{d^d k_i}{i\pi^{\frac{d}{2}}} e^{\epsilon\gamma_E} \left( \frac{m_V^2}{\mu^2} \right)^\epsilon. \quad (4.3)$$

The number of master integrals for the planar topology (P) is 48, while for the non-planar topology (NP) we found 61 master integrals. The MIs relevant for this process have been analytically computed in [46] and [47], respectively for the planar and non-planar topologies. For the purpose of this project we performed an independent numerical computation based on the generalized series expansion method described in [48]. The MIs basis, the differential equation matrices and the boundary values are given in the ancillary

files, along with the scalar form-factors and the relevant tensor structures. The numerical evaluation is performed with a private implementation of the method [48], however it is possible to use the material given in the ancillary files also within the software DIFFEXP [49].

#### 4.1 Differential equations approach

The MIs satisfy a system of linear first order partial differential equations with respect to the kinematic invariants [63, 72]. In order to solve the system efficiently we adopted the canonical basis approach [62, 73]. A set of MIs  $\vec{f}(\vec{x}, \varepsilon)$  is said to be in canonical form if it satisfies a system of differential equations of the kind:

$$d\vec{f}(\vec{x}, \varepsilon) = \varepsilon \sum_i A_i(\vec{x}) \vec{f}(\vec{x}, \varepsilon) dx_i, \quad A_i(\vec{x}) := \partial_{x_i} \tilde{A}(\vec{x}), \quad (4.4)$$

where  $\varepsilon$  is the dimensional regularization parameter and  $d$  is the total differential with respect to the kinematic invariants  $\vec{x}$ . The matrix  $\tilde{A}(\vec{x})$  is a  $\mathbb{Q}$ -linear combination of logarithms,

$$\tilde{A}(\vec{x}) = \sum_i c_i \log(\alpha_i(\vec{x})), \quad (4.5)$$

where  $c_i$  are matrices of rational numbers and  $\alpha_i(\vec{x})$  are algebraic functions of the kinematic invariants which we refer to as *letters*. The set of letters is usually called the *alphabet*. For the planar (non-planar) topology we find 25 (62) independent letters, such that

$$\sum_i^{25, (62)} c_i d \log(\alpha_i(\vec{x})) = 0 \quad \Rightarrow \quad c_i = 0 \quad \forall i, \quad (4.6)$$

which involve the square roots

$$\begin{aligned} r_1 &= \sqrt{-m_H^2} \sqrt{4m_V^2 - m_H^2}, \\ r_2 &= \sqrt{s - m_H^2} \sqrt{-m_H^2 + 4m_V^2 + s}, \\ r_3 &= \sqrt{-t} \sqrt{4m_V^2(s+t)(m_H^2 - s) - tm_H^4}, \\ r_4 &= \sqrt{-m_H^2 + s + t} \sqrt{4m_V^2(m_H^2 - s)(m_H^2 - t) + m_H^4(-m_H^2 + s + t)}, \end{aligned} \quad (4.7)$$

where  $s = (p_1 + p_2)^2$  and  $t = (p_1 - p_3)^2$ . The alphabet for the planar and non-planar topologies is provided as part of the ancillary material.

In order to find a canonical basis several approaches have been proposed [74–80]. We choose the approach discussed in [81, 82]. The system of differential equations eq. (4.4) admits the solution in terms of Chen iterated integrals [83],

$$\vec{f}(\vec{x}, \varepsilon) = \mathbb{P} \exp \left( \varepsilon \int_{\gamma} d\tilde{A}(\vec{x}) \right) \vec{f}(\vec{x}_0, \varepsilon), \quad (4.8)$$



where  $\mathbb{P}$  is the path-ordering operator,  $\gamma$  represents a path in kinematic space and  $\vec{f}(\vec{x}_0, \varepsilon)$  is the vector of boundary conditions. In the context of high-energy physics, the solution eq. (4.8) is written as a series expansion with respect to the dimensional regularization parameter around the point  $\varepsilon = 0$ ,

$$\vec{f}(\vec{x}, \varepsilon) = \sum_{k=0}^{\infty} \varepsilon^k \vec{f}^{(k)}(\vec{x}) \quad (4.9)$$

The coefficients of the expansion can be explicitly written, for example, parametrizing the integration path  $\gamma$  with a parameter  $t \in [0, 1]$ :

$$\vec{f}(\vec{x}, \varepsilon) = \vec{f}^{(0)}(\vec{x}_0) + \sum_{k=1}^{\infty} \varepsilon^k \sum_{j=1}^k \int_0^1 dt_1 A(t_1) \int_0^{t_1} dt_2 A(t_2) \cdots \int_0^{t_{j-1}} dt_j A(t_j) \vec{f}^{(k-j)}(\vec{x}_0), \quad (4.10)$$

where the matrices  $A(t)$  denote the pull-back onto the interval  $[0, t]$  along the path  $\gamma$ :

$$A(t)dt := \gamma^*(d\vec{A}(\vec{x}))(t). \quad (4.11)$$

The alphabet of the system of differential equations determines the functional space in which the solution to eq. (4.4) is represented. Specifically, if the  $\alpha_i(\vec{x})$  are rational in the kinematic invariants, it is possible to write eq. (4.10) order-by-order in  $\varepsilon$  in terms of MPLs [84, 85],

$$G(w_1, \dots, w_n; z) = \int_0^z \frac{dt}{t - w_1} G(w_2, \dots, w_n; z), \quad (4.12)$$

with

$$G(; z) = 1, \quad G(\vec{0}; z) \equiv \frac{\log^n z}{n!}. \quad (4.13)$$

For algebraic  $\alpha_i(\vec{x})$  in eq. (4.5), it is not always possible to write the solution of eq. (4.4) in terms of MPLs [86]. However, in certain cases one can obtain a representation in terms of MPLs by employing computational techniques involving the *symbol* associated to the solution itself [32, 87, 88]. Such is the case of both the planar and the non-planar topologies of the two-loop  $gg \rightarrow Hg$  amplitude [46, 47], for which a representation in terms of MPLs can be achieved, despite the fact that the system of differential equations depends on the set of square roots eq. (4.7).

## 4.2 Series expansion method

In our computation of the mixed QCD-EW cross section [1], we did not aim at a fully analytic two-loop  $gg \rightarrow Hg$  amplitude as in [47]. Instead we exploited the method of generalized power series [48] to evaluate the MIs numerically in the physical phase-space regions. In the following paragraph, we want to review the main points of this semi-analytical integration.

The method can be summarised as follows: given the knowledge of the solution of the system eq. (4.4) in a given point  $\vec{x}_0$  (either analytically or numerically with high-precision),

it is possible to evaluate the solution in a point  $\vec{x}_a$  numerically, by patching together local solutions in terms of generalized power series. The advantages of this strategy are several. First, it allows to obtain high-precision numerical results for a system of MIs regardless of the actual space of functions in which the analytic solution may be expressed. This aspect is particularly relevant when dealing with Feynman integrals that admit a solution in terms of elliptic integrals [32–34], for which the numerical evaluation of analytic expression has received, recently, increasing attention [89–91]. Secondly, even if the solution can be expressed in terms of MPLs it can be more convenient, especially for phenomenological applications [1, 92], to exploit this generalized power series method. In particular when the system of differential equations involves square roots of the kinematic invariants, the numerical evaluation of an analytic solution expressed in terms of MPLs can be less efficient and it involves complicated analytic continuation for the special functions.

We assume that the solution to the system eq. (4.4) is known in a point  $\vec{x}_0$  and we want to evaluate it at a point  $\vec{x}_a$ . The system eq. (4.4) can be written with respect to some variable  $t$  which parametrizes the path  $\gamma(t)$  that connects the points  $\vec{x}_0$  and  $\vec{x}_a$ :

$$\gamma(t) : t \mapsto \vec{x}(t), \quad t \in [0, 1], \quad \gamma(0) = \vec{x}_0, \quad \gamma(1) = \vec{x}_a. \quad (4.14)$$

As already shown in eq. (4.10), the solution can be written as

$$\vec{f}(t, \varepsilon) = \sum_{k=0}^{\infty} \varepsilon^k \vec{f}^{(k)}(t), \quad (4.15)$$

$$\vec{f}^{(k)}(t) = \sum_{j=1}^k \int_0^1 dt_1 A(t_1) \int_0^{t_1} dt_2 A(t_2) \cdots \int_0^{t_{j-1}} dt_j A(t_j) \vec{f}^{(k-j)}(\vec{x}_0) + \vec{f}^{(k)}(\vec{x}_0). \quad (4.16)$$

The first step is to split the path which connects the points  $\vec{x}_0$  and  $\vec{x}_a$  into segments  $S_i := [t_i - r_i, t_i + r_i)$ . Then, inside each segment  $S_i$ , we denote by  $\vec{f}_i^{(k)}(t)$  the local solution obtained as a truncated power series expansion around  $t_i$  with radius of convergence  $r_i$ . The global solution on the path  $\gamma(t)$  can then be approximated as:

$$\vec{f}(t, \varepsilon) = \sum_{k=0}^{\infty} \varepsilon^k \sum_{i=0}^{N-1} \rho_i(t) \vec{f}_i^{(k)}(t), \quad \rho(t) = \begin{cases} 1, & t \in [t_i - r_i, t_i + r_i) \\ 0, & t \notin [t_i - r_i, t_i + r_i) \end{cases}, \quad (4.17)$$

where  $N$  is the total number of segments.

We can construct the segments  $S_i$  from the knowledge of the singular points of the differential equations. In the general case, we can have both real and complex-valued singular points. Let us denote the real singular points of the system of differential equations as  $R := \{\tau_i \mid i = 1, \dots, N_r\}$ , and the complex-valued ones as  $C := \{\lambda_i^{re} + i\lambda_i^{im} \mid i = 1, \dots, N_c\}$ . Starting from  $C$  we can construct a set of regular points  $C_r := \cup_{i=1}^{N_c} \{\lambda_i^{re} \pm \lambda_i^{im}\}$ , therefore we can choose the expansion points  $t_i$ , which define the segments  $S_i$ , to belong to the set  $R \cup C_r$ , and the radius of convergence  $r_i$  can be defined as the distance of  $t_i$  to the closest element  $t_p$ , with  $p \neq i$ .

As a second step we need to know the local solution inside each segment  $S_i$ . This can be done by expanding the system of differential equations around the point  $t_i$ :

$$A(t) = \sum_{l=0}^{\infty} A_l (t - t_i)^{w_l}, \quad w_l \in \mathbb{Q}, \quad (4.18)$$

where  $A_l$  are constant matrices. By substituting eq. (4.18) into  $\vec{f}_i^{(k)}(t)$  we obtain:

$$\begin{aligned} \vec{f}_i^{(k)}(t) = & \sum_{j=1}^k \sum_{l_1=0}^{\infty} \cdots \sum_{l_j=0}^{\infty} A_{l_1} \cdots A_{l_j} \int_0^t dt_1 (t_1 - t_i)^{w_{l_1}} \cdots \int_0^{t_{j-1}} dt_j (t_j - t_i)^{w_{l_j}} \vec{f}_i^{(k-j)}(\vec{x}_0) \\ & + \vec{f}_i^{(k)}(\vec{x}_0). \end{aligned} \quad (4.19)$$

As a consequence of working with a system of differential equations in canonical form, the integrals that appear in eq. (4.19) are of the form:

$$\int_0^{t_0} dt (t - t_i)^w \log(t - t_i)^m, \quad w \in \mathbb{Q}, \quad m \in \mathbb{N}, \quad (4.20)$$

this implies that eq. (4.19) can be written as

$$\vec{f}_i^{(k)}(t) = \sum_{l_1=0}^{\infty} \sum_{l_2=0}^{N_{i,k}} c_k^{(i,l_1,l_2)} (t - t_i)^{\frac{l_1}{2}} \log(t - t_i)^{l_2}, \quad (4.21)$$

where the rational exponent  $\frac{l_1}{2}$  is a consequence of the presence of the square roots, e. g. eq. (4.7), in the system of differential equations. The matrices  $c_k^{(i,l_1,l_2)}$  depend on the boundary conditions and the constant matrices  $A_l$  in eq. (4.18). Finally, using the previous result for  $\vec{f}_i^{(k)}(t)$ , it is possible to numerically evaluate the solution in the point  $\vec{x}_a$  by employing the expression eq. (4.17).

We conclude this brief review of the method by emphasizing that the endpoint of the integration path is considered a fixed numerical value so that the result is not considered a function of the endpoint itself, as for example in fully analytic approaches.

### 4.3 Analytic continuation

Let us now turn to the analytic continuation, which in this approach simply means a singularity of the matrix  $A(t)$  exists for  $t \in [0, 1]$  such that the contour will cross a branch-cut. In eq. (4.21) it is obvious that we will need to analytically continue only roots (typically square roots) and logarithms. For physical thresholds  $s_{phys.}$ , which are linear in one kinematic variable  $x_k$ , Feynman prescription dictates to assign a small positive imaginary part  $i\eta$ , such that

$$x_k(t) = a + bt \mapsto a + bt + i\eta \quad \Rightarrow \quad x_k(t) \mapsto x_k(t + i\text{sign}(b)\eta). \quad (4.22)$$

This directly determines the imaginary part for the logarithms of the series around the threshold. More subtle are the singularities of the differential equations which are multivariate polynomials in the kinematic invariants. For these singularities, an analytic continuation can be very non-trivial often. However, if these singularities are spurious the analytic continuation for intermediate steps does not matter. We say, a singularity is spurious if all the numeric coefficient  $c_k^{(i,l_1,l_2)}$  in eq. (4.21) vanish identically; the Feynman integral does not depend on these logarithms at all. This can be turned into an efficient check. We assume that all multivariate polynomial singularities are spurious. Then we check explicitly, for each integration, that indeed all numeric coefficients vanish whenever a contour crosses such singularities.

The analytic continuation for “physical square roots” (linear in one kinematic invariant) is completely analogous. However, a sufficient condition for a square-root to be spurious does not only involve the vanishing of the numeric coefficients  $c$  in eq. (4.21). This is due to the algebraic transformation we use to obtain a canonical basis  $\vec{f}$  from a basis of scalar integrals  $\vec{\mathcal{J}}$

$$\vec{f} = T(\vec{x}, \varepsilon) \vec{\mathcal{J}}. \quad (4.23)$$

For a square root to be spurious all coefficients in front of that root have to vanish for all  $\mathcal{J}_i \in \vec{\mathcal{J}}$ . So whenever a contour crosses an assumed spurious branch-cut of a root, one has to invert back to the scalar integrals  $\vec{\mathcal{J}}$  and verify that indeed all coefficients in front of the root vanish for all scalar Feynman integrals. For logarithms, this is not necessary since they will never be used in the transformations to obtain a canonical basis.

#### 4.4 Boundary conditions

In order to evaluate the semi-analytic integration we obtain the initial boundary value in the large boson mass limit  $m_V^2 \gg |m_H^2|, |s|, |t|$  when approached along a straight line from the un-physical region  $m_H^2, s, t < 0$ . In this limit, only a subset of factorized one-loop and sunrise-type integrals contribute. In particular, we compute the integrals:

$$\begin{array}{cccc} \mathcal{J}_{000210200}^{(NP)}, & \mathcal{J}_{000211000}^{(NP)}, & \mathcal{J}_{000220100}^{(NP)}, & \mathcal{J}_{002012000}^{(NP)}, \\ \mathcal{J}_{002021000}^{(NP)}, & \mathcal{J}_{020100200}^{(NP)}, & \mathcal{J}_{020200100}^{(NP)}, & \mathcal{J}_{021000200}^{(NP)}, \\ \mathcal{J}_{022000100}^{(NP)}, & \mathcal{J}_{200100200}^{(NP)}, & \mathcal{J}_{200101200}^{(NP)} & \end{array} \quad (4.24)$$

and respectively:

$$\begin{array}{cccc} \mathcal{J}_{000210200}^{(P)}, & \mathcal{J}_{000220100}^{(P)}, & \mathcal{J}_{002010200}^{(P)}, & \mathcal{J}_{020012000}^{(P)}, \\ \mathcal{J}_{020021000}^{(P)}, & \mathcal{J}_{021000200}^{(P)}, & \mathcal{J}_{022000100}^{(P)}, & \mathcal{J}_{101110200}^{(P)}, \\ \mathcal{J}_{200100200}^{(P)}, & \mathcal{J}_{210000100}^{(P)}, & \mathcal{J}_{210002000}^{(P)}, & \mathcal{J}_{220001000}^{(P)} \end{array} \quad (4.25)$$

exactly and augment them with the large mass expansion of:

$$\mathcal{J}_{101112000}^{(NP)}, \quad \mathcal{J}_{101121000}^{(NP)}, \quad \mathcal{J}_{111100200}^{(NP)}, \quad \mathcal{J}_{121100100}^{(NP)} \quad (4.26)$$

and:

$$\mathcal{J}_{111012000}^{(P)}, \quad \mathcal{J}_{111100200}^{(P)}, \quad \mathcal{J}_{121011000}^{(P)}, \quad \mathcal{J}_{121100100}^{(P)} \quad (4.27)$$

respectively. The large mass expansion is performed by means of an expansion by regions with help of the code ASY [93]. The boundary conditions are included in the ancillary file.

## 5 Conclusions

The two-loop amplitude described in this work has been used for our computation of the light-quark contribution to the NLO-mixed QCD-electroweak contribution to the gluon fusion Higgs production cross section [1]. This means, in particular, that our result is aimed at sufficiently fast, high-precision, numerical evaluations in the complete physical phase-space and it motivates our choice of the semi-analytic integration discussed in section 4.2. In order to perform the integration we use a private implementation of the algorithm [48]. In particular, to facilitate the cross section computation, we have pre-computed a grid of values obtained by an analogous  $gg \rightarrow Hg$ -HEFT computation. This means that our starting grid is non-uniform and much more dense near the IR-singular regions.

The evaluation of the  $\sim 300$  canonical integrals (including crossing), takes on average  $\sim 1$  min on a single CPU thread. For phase-space points very close to the IR-singular configuration or deep in the UV the evaluation time increases considerably to  $\sim 5 - 15$  min. In these regions, the scale hierarchies become extreme and higher depth expansions are needed in order to reach a fixed precision of better than 16-digits.

In order to perform the cross section computation [1] we integrated the amplitude into MADGRAPH5\_AMC@NLO program [94], allowing for the generation of a standalone library for the evaluation of all matrix elements entering the computation, by means of a dedicated plugin<sup>4</sup> detailed in appendix A.

We furthermore provide ancillary files for the differential equations, the boundary conditions and the amplitude, which allows a standalone evaluation of the amplitude within the publicly available code DIFFEXP [49].

## 6 Acknowledgements

The authors are grateful to Roberto Bonciani and Vittorio del Duca for useful inputs and discussions throughout the project. We also thank Valerio Casconi for the valuable work

---

<sup>4</sup>available under

[https://bitbucket.org/aschweitzer/mg5\\_higgs\\_ew\\_plugin/](https://bitbucket.org/aschweitzer/mg5_higgs_ew_plugin/)

or

<http://madgraph.physics.illinois.edu/Downloads/PLUGIN/higgsew.tar.gz>

in the early stage of the computation. M.B. also acknowledges the financial support from the European Union Horizon 2020 research and innovation programme: High precision multi-jet dynamics at the LHC (grant agreement no. 772009).

## A Example usage of the dedicated MadGraph5\_aMC@NLO-plugin

The  $A_{gg \rightarrow Hg}^{\text{QCD-EW}}$ -amplitude contributes to a pure NLO-QCD correction, even though the LO is at two-loops. In particular, this means it is suited for a fully automatized treatment in publicly available NLO matrix element generators. For the cross section computation [1], we implemented our amplitude as a plugin into the MADGRAPH5\_AMC@NLO programme [94], which we will abbreviate as MG5AMC. In the MG5AMC-framework Feynman rules are implemented in the Universal FeynRules Output (UFO) [95] model. The UFO is a representation of a vertex  $v$  in the following universal form

$$v(\text{fields, momenta}) = \sum_i \sum_j (\text{color fact.})_i \times (\text{Lorentz struct.})_j \times (\text{coupling const.})_{ij}. \quad (\text{A.1})$$

In the usual pipeline this representation is derived directly from the Lagrangian with the FeynRules-package. In MG5AMC this representation is used as follows. One defines the process and specifies the coupling order. Then all valid amplitudes at the specified coupling order are build, the Feynman rules get inserted and the resulting expression auto-generates FORTRAN code for the numerical evaluation with the help of ALOHA [96]. Each matrix-element becomes a standalone FORTRAN-library that is used for all successive computations.

The UFO-model is our entry point into this pipeline. All color-decomposed, tensor-projected amplitudes define an effective vertex where the coupling constants are the scalar form-factors. The only difference w.r.t. to the tree-level UFO-representation is that our coupling constant gets dynamically updated at each phase-space point. We define for each mixed QCD-EW  $A_{gg \rightarrow H}^{\text{QCD-EW}}$ ,  $A_{gg \rightarrow H}^{\text{QCD-EW}}$ ,  $A_{gg \rightarrow H+g}^{\text{QCD-EW}}$ , and for each HEFT-amplitude  $A_{gg \rightarrow H}^{\text{HEFT}}$ ,  $A_{gg \rightarrow H}^{\text{HEFT}}$ ,  $A_{gg \rightarrow H+g}^{\text{HEFT}}$  an effective vertex. The virtual mixed QCD-EW amplitudes are taken from [44, 97]. For performance reasons we fix the Higgs and the electroweak-boson masses such that the virtual amplitudes are just a number<sup>5</sup>. The HEFT-amplitude  $A_{gg \rightarrow H+g}^{\text{HEFT}}$  is a pure-Lorentz structure, and only the mixed amplitude  $A_{gg \rightarrow H+g}^{\text{QCD-EW}}$  is a costly coupling computation at each phase-space point.

---

<sup>5</sup>We validate that the input parameters correspond to our fixed values. E. g. when our implementation is run with masses different to these values, it will abort and inform the user. However, we provide these coupling calls as templates such that arbitrary mass-dependent computations can be performed with very minor modifications of the code.

After following the installation instructions<sup>6</sup> one can for example use our plugin with

```
#
# start mg5_aMC with our plugin
#
python2 ./mg5_aMC --mode=higgsew
#
# information on coupling parameters gets printed
#
GGHG.Interface: PLUGIN INFORMATION:
GGHG.Interface: -----
GGHG.Interface: HEFT QCD-Background:
GGHG.Interface: -----
GGHG.Interface: For LO:
GGHG.Interface: generate g g > H   GGHEFT^2==2   QCD^2==4
GGHG.Interface: generate g g > H g   GGGHEFT^2==2   QCD^2==6
GGHG.Interface: For NLO-virtuals:
GGHG.Interface: generate g g > H   GGHEFT^2==2   QCD^2==6
GGHG.Interface: -----
GGHG.Interface: Massive Mixed EW:
GGHG.Interface: -----
GGHG.Interface: For LO:
GGHG.Interface: generate g g > H   GGHEFT^2==1   GGHEW^2==1   QCD^2==4
GGHG.Interface: generate g g > H g   GGGHEFT^2==1   GGGHEW^2==1   QCD^2==6
GGHG.Interface: For NLO-virtuals:
GGHG.Interface: generate g g > H   GGHEFT^2==1   GGHEW^2==1   QCD^2==6
GGHG.Interface: -----
GGHG.Interface: OUTPUT
GGHG.Interface: -----
GGHG.Interface: use: output standalone-ggHg OUTPUTDIR
```

The generation statements are directly related to the UFO-representation. One defines a process and a coupling order. For example, for the HEFT-amplitudes we see the definition

```
GGHG.Interface: For LO:
GGHG.Interface: generate g g > H   GGHEFT^2==2   QCD^2==4
```

The *generate g g > H* command defines the process, and  $\text{GGHEFT}^2==2 \text{ QCD}^2==4$  specifies that we are working at  $C_{\text{Wilson}}^2$  and  $g_s^4$ . If we want one higher order in QCD, e.g. the virtuals, we need to increase to  $\text{QCD}^2==6$  but retain the count of the Wilson coefficient. If we interfere against non-HEFT amplitudes, the squared Wilson coefficient count is decreased to  $\text{GGHEFT}^2==1$ , e.g. only one of the interfered amplitudes involves a HEFT-coupling. One is now in the default MG5aMC command line environment and can generate all processes. For example, typing

```
MG5_aMC> generate g g > H g   GGGHEFT^2==1 GGGHEW^2==1 QCD^2==6
#
# printed info on amplitude
```

---

<sup>6</sup>available under

[https://bitbucket.org/aschweitzer/mg5\\_higgs\\_ew\\_plugin/](https://bitbucket.org/aschweitzer/mg5_higgs_ew_plugin/)

or

<http://madgraph.physics.illinois.edu/Downloads/PLUGIN/higgsew.tar.gz>

```
#  
INFO: Process has 3 diagrams
```

will generate the amplitudes for the interferences of the real radiation diagrams, where `MG5_aMC` is just the prompt of the interface. The three diagrams are the HEFT-amplitude and the mixed QCD-EW amplitudes for the two different masses  $m_{W/Z}$ . In order to compile the process into a standalone library one needs to specify an output directory

```
MG5_aMC>output standalone_ggHg example_gghg_standalone
```

This output directory “*example\_gghg\_standalone*” includes, among other things, a standalone library for the numerical evaluation of the matrix elements. This means, one can perform the cross section computation with any public or private code by linking against this library. Since our scalar integrals are evaluated in MATHEMATICA, which provides a poor interface with low-level languages, we perform an offline-parallelisation over the Monte-Carlo grids of the cross section computation. Sample codes which can be used to facilitate such an offline parallelization are provided with the plugin.



## References

- [1] M. Becchetti, R. Bonciani, V. Del Duca, V. Hirschi, F. Moriello, and A. Schweitzer, *Next-to-leading order corrections to light-quark mixed QCD-EW contributions to Higgs boson production*, *Phys. Rev. D* **103** (2021), no. 5 054037, [[2010.09451](#)].
- [2] **ATLAS** Collaboration, G. Aad *et al.*, *Observation of a new particle in the search for the Standard Model Higgs boson with the ATLAS detector at the LHC*, *Phys.Lett.* **B716** (2012) 1–29, [[1207.7214](#)].
- [3] **CMS** Collaboration, S. Chatrchyan *et al.*, *Observation of a new boson at a mass of 125 GeV with the CMS experiment at the LHC*, *Phys.Lett.* **B716** (2012) 30–61, [[1207.7235](#)].
- [4] H. Georgi, S. Glashow, M. Machacek, and D. V. Nanopoulos, *Higgs Bosons from Two Gluon Annihilation in Proton Proton Collisions*, *Phys. Rev. Lett.* **40** (1978) 692.
- [5] D. Graudenz, M. Spira, and P. M. Zerwas, *QCD corrections to Higgs boson production at proton proton colliders*, *Phys. Rev. Lett.* **70** (1993) 1372–1375.
- [6] M. Spira, A. Djouadi, D. Graudenz, and P. M. Zerwas, *Higgs boson production at the LHC*, *Nucl. Phys.* **B453** (1995) 17–82, [[hep-ph/9504378](#)].
- [7] R. V. Harlander and W. B. Kilgore, *Next-to-next-to-leading order Higgs production at hadron colliders*, *Phys. Rev. Lett.* **88** (2002) 201801, [[hep-ph/0201206](#)].
- [8] C. Anastasiou and K. Melnikov, *Higgs boson production at hadron colliders in NNLO QCD*, *Nucl. Phys.* **B646** (2002) 220–256, [[hep-ph/0207004](#)].
- [9] V. Ravindran, J. Smith, and W. L. van Neerven, *NNLO corrections to the total cross-section for Higgs boson production in hadron hadron collisions*, *Nucl. Phys.* **B665** (2003) 325–366, [[hep-ph/0302135](#)].
- [10] C. Anastasiou, C. Duhr, F. Dulat, and B. Mistlberger, *Soft triple-real radiation for Higgs production at N<sup>3</sup>LO*, *JHEP* **07** (2013) 003, [[1302.4379](#)].
- [11] C. Anastasiou, C. Duhr, F. Dulat, F. Herzog, and B. Mistlberger, *Real-virtual contributions to the inclusive Higgs cross-section at N<sup>3</sup>LO*, *JHEP* **12** (2013) 088, [[1311.1425](#)].
- [12] C. Anastasiou, C. Duhr, F. Dulat, E. Furlan, T. Gehrmann, F. Herzog, and B. Mistlberger, *Higgs Boson GluonFusion Production Beyond Threshold in N<sup>3</sup>LO QCD*, *JHEP* **03** (2015) 091, [[1411.3584](#)].
- [13] Y. Li, A. von Manteuffel, R. M. Schabinger, and H. X. Zhu, *Soft-virtual corrections to Higgs production at N<sup>3</sup>LO*, *Phys. Rev.* **D91** (2015) 036008, [[1412.2771](#)].
- [14] C. Anastasiou, C. Duhr, F. Dulat, F. Herzog, and B. Mistlberger, *Higgs Boson Gluon-Fusion Production in QCD at Three Loops*, *Phys. Rev. Lett.* **114** (2015) 212001, [[1503.06056](#)].
- [15] B. Mistlberger, *Higgs boson production at hadron colliders at N<sup>3</sup>LO in QCD*, *JHEP* **05** (2018) 028, [[1802.00833](#)].
- [16] C. Anastasiou, C. Duhr, F. Dulat, E. Furlan, T. Gehrmann, F. Herzog, A. Lazopoulos, and B. Mistlberger, *High precision determination of the gluon fusion Higgs boson cross-section at the LHC*, *JHEP* **05** (2016) 058, [[1602.00695](#)].

- [17] C. Anastasiou, S. Beerli, S. Bucherer, A. Daleo, and Z. Kunszt, *Two-loop amplitudes and master integrals for the production of a Higgs boson via a massive quark and a scalar-quark loop*, *JHEP* **01** (2007) 082, [[hep-ph/0611236](#)].
- [18] A. Pak, M. Rogal, and M. Steinhauser, *Finite top quark mass effects in NNLO Higgs boson production at LHC*, *JHEP* **02** (2010) 025, [[0911.4662](#)].
- [19] R. V. Harlander, H. Mantler, S. Marzani, and K. J. Ozeren, *Higgs production in gluon fusion at next-to-next-to-leading order QCD for finite top mass*, *Eur. Phys. J.* **C66** (2010) 359–372, [[0912.2104](#)].
- [20] R. V. Harlander and K. J. Ozeren, *Finite top mass effects for hadronic Higgs production at next-to-next-to-leading order*, *JHEP* **11** (2009) 088, [[0909.3420](#)].
- [21] R. V. Harlander, T. Neumann, K. J. Ozeren, and M. Wiesemann, *Top-mass effects in differential Higgs production through gluon fusion at order  $\alpha_s^4$* , *JHEP* **08** (2012) 139, [[1206.0157](#)].
- [22] M. Czakon, R. V. Harlander, J. Klappert, and M. Niggetiedt, *Exact Top-Quark Mass Dependence in Hadronic Higgs Production*, *Phys. Rev. Lett.* **127** (2021), no. 16 162002, [[2105.04436](#)].
- [23] R. Harlander and P. Kant, *Higgs production and decay: Analytic results at next-to-leading order QCD*, *JHEP* **0512** (2005) 015, [[hep-ph/0509189](#)].
- [24] U. Aglietti, R. Bonciani, G. Degrossi, and A. Vicini, *Analytic Results for Virtual QCD Corrections to Higgs Production and Decay*, *JHEP* **01** (2007) 021, [[hep-ph/0611266](#)].
- [25] R. Bonciani, G. Degrossi, and A. Vicini, *Scalar particle contribution to Higgs production via gluon fusion at NLO*, *JHEP* **11** (2007) 095, [[0709.4227](#)].
- [26] C. Anastasiou, S. Bucherer, and Z. Kunszt, *HPro: A NLO Monte-Carlo for Higgs production via gluon fusion with finite heavy quark masses*, *JHEP* **10** (2009) 068, [[0907.2362](#)].
- [27] C. Anastasiou, N. Deuschmann, and A. Schweitzer, *Quark mass effects in two-loop Higgs amplitudes*, *JHEP* **07** (2020) 113, [[2001.06295](#)].
- [28] C. Anastasiou and A. Penin, *Light Quark Mediated Higgs Boson Threshold Production in the Next-to-Leading Logarithmic Approximation*, *JHEP* **07** (2020) 195, [[2004.03602](#)]. [Erratum: *JHEP* 01, 164 (2021)].
- [29] R. V. Harlander, M. Prausa, and J. Usovitsch, *The light-fermion contribution to the exact Higgs-gluon form factor in QCD*, *JHEP* **10** (2019) 148, [[1907.06957](#)]. [Erratum: *JHEP* 08, 101 (2020)].
- [30] M. L. Czakon and M. Niggetiedt, *Exact quark-mass dependence of the Higgs-gluon form factor at three loops in QCD*, *JHEP* **05** (2020) 149, [[2001.03008](#)].
- [31] M. Prausa and J. Usovitsch, *The analytic leading color contribution to the Higgs-gluon form factor in QCD at NNLO*, *JHEP* **03** (2021) 127, [[2008.11641](#)].
- [32] R. Bonciani, V. Del Duca, H. Frellesvig, J. M. Henn, F. Moriello, and V. A. Smirnov, *Two-loop planar master integrals for Higgs  $\rightarrow$  3 partons with full heavy-quark mass dependence*, *JHEP* **12** (2016) 096, [[1609.06685](#)].

- [33] R. Bonciani, V. Del Duca, H. Frellesvig, J. M. Henn, M. Hidding, L. Maestri, F. Moriello, G. Salvatori, and V. A. Smirnov, *Evaluating a family of two-loop non-planar master integrals for Higgs + jet production with full heavy-quark mass dependence*, *JHEP* **01** (2020) 132, [[1907.13156](#)].
- [34] H. Frellesvig, M. Hidding, L. Maestri, F. Moriello, and G. Salvatori, *The complete set of two-loop master integrals for Higgs + jet production in QCD*, *JHEP* **06** (2020) 093, [[1911.06308](#)].
- [35] V. Del Duca, W. Kilgore, C. Oleari, C. Schmidt, and D. Zeppenfeld, *Gluon fusion contributions to  $H + 2$  jet production*, *Nucl. Phys. B* **616** (2001) 367–399, [[hep-ph/0108030](#)].
- [36] L. Budge, J. M. Campbell, G. De Laurentis, R. K. Ellis, and S. Seth, *The one-loop amplitudes for Higgs + 4 partons with full mass effects*, *JHEP* **05** (2020) 079, [[2002.04018](#)].
- [37] U. Aglietti, R. Bonciani, G. Degrassi, and A. Vicini, *Two loop light fermion contribution to Higgs production and decays*, *Phys.Lett.* **B595** (2004) 432–441, [[hep-ph/0404071](#)].
- [38] U. Aglietti, R. Bonciani, G. Degrassi, and A. Vicini, *Master integrals for the two-loop light fermion contributions to  $gg \rightarrow H$  and  $H \rightarrow \gamma\gamma$* , *Phys. Lett.* **B600** (2004) 57–64, [[hep-ph/0407162](#)].
- [39] G. Degrassi and F. Maltoni, *Two-loop electroweak corrections to Higgs production at hadron colliders*, *Phys. Lett.* **B600** (2004) 255–260, [[hep-ph/0407249](#)].
- [40] S. Actis, G. Passarino, C. Sturm, and S. Uccirati, *NLO Electroweak Corrections to Higgs Boson Production at Hadron Colliders*, *Phys. Lett.* **B670** (2008) 12–17, [[0809.1301](#)].
- [41] V. Hirschi, S. Lionetti, and A. Schweitzer, *One-loop weak corrections to Higgs production*, *JHEP* **05** (2019) 002, [[1902.10167](#)].
- [42] C. Anastasiou, R. Boughezal, and F. Petriello, *Mixed QCD-electroweak corrections to Higgs boson production in gluon fusion*, *JHEP* **04** (2009) 003, [[0811.3458](#)].
- [43] M. Bonetti, K. Melnikov, and L. Tancredi, *Two-loop electroweak corrections to Higgs–gluon couplings to higher orders in the dimensional regularization parameter*, *Nucl. Phys. B* **916** (2017) 709–726, [[1610.05497](#)].
- [44] M. Bonetti, K. Melnikov, and L. Tancredi, *Higher order corrections to mixed QCD-EW contributions to Higgs boson production in gluon fusion*, *Phys. Rev. D* **97** (2018), no. 5 056017, [[1801.10403](#)]. [Erratum: *Phys.Rev.D* 97, 099906 (2018)].
- [45] C. Anastasiou, V. del Duca, E. Furlan, B. Mistlberger, F. Moriello, A. Schweitzer, and C. Specchia, *Mixed QCD-electroweak corrections to Higgs production via gluon fusion in the small mass approximation*, *JHEP* **03** (2019) 162, [[1811.11211](#)].
- [46] M. Becchetti, R. Bonciani, V. Casconi, V. Del Duca, and F. Moriello, *Planar master integrals for the two-loop light-fermion electroweak corrections to Higgs plus jet production*, *JHEP* **12** (2018) 019, [[1810.05138](#)].
- [47] M. Bonetti, E. Panzer, V. A. Smirnov, and L. Tancredi, *Two-loop mixed QCD-EW corrections to  $gg \rightarrow Hg$* , *JHEP* **11** (2020) 045, [[2007.09813](#)].

- [48] F. Moriello, *Generalised power series expansions for the elliptic planar families of Higgs + jet production at two loops*, [1907.13234](#).
- [49] M. Hidding, *DiffExp, a Mathematica package for computing Feynman integrals in terms of one-dimensional series expansions*, *Comput. Phys. Commun.* **269** (2021) 108125, [[2006.05510](#)].
- [50] J. Ellis, *TikZ-Feynman: Feynman diagrams with TikZ*, *Comput. Phys. Commun.* **210** (2017) 103–123, [[1601.05437](#)].
- [51] P. Nogueira, *Automatic Feynman graph generation*, *J. Comput. Phys.* **105** (1993) 279–289.
- [52] K. G. Chetyrkin and F. V. Tkachov, *Integration by Parts: The Algorithm to Calculate beta Functions in 4 Loops*, *Nucl. Phys.* **B192** (1981) 159–204.
- [53] P. Maierhöfer, J. Usovitsch, and P. Uwer, *Kira—A Feynman integral reduction program*, *Comput. Phys. Commun.* **230** (2018) 99–112, [[1705.05610](#)].
- [54] P. Maierhöfer and J. Usovitsch, *Kira 1.2 Release Notes*, [1812.01491](#).
- [55] J. C. Collins, *Renormalization: An Introduction to Renormalization, the Renormalization Group and the Operator-Product Expansion*. Cambridge Monographs on Mathematical Physics. Cambridge University Press, 1984.
- [56] T. Peraro and L. Tancredi, *Physical projectors for multi-leg helicity amplitudes*, *JHEP* **07** (2019) 114, [[1906.03298](#)].
- [57] T. Peraro and L. Tancredi, *Tensor decomposition for bosonic and fermionic scattering amplitudes*, *Phys. Rev. D* **103** (2021), no. 5 054042, [[2012.00820](#)].
- [58] L. Chen, *A prescription for projectors to compute helicity amplitudes in D dimensions*, [1904.00705](#).
- [59] S. Abreu, F. Febres Cordero, H. Ita, B. Page, and V. Sotnikov, *Planar Two-Loop Five-Parton Amplitudes from Numerical Unitarity*, *JHEP* **11** (2018) 116, [[1809.09067](#)].
- [60] E. W. N. Glover, *Two loop QCD helicity amplitudes for massless quark quark scattering*, *JHEP* **04** (2004) 021, [[hep-ph/0401119](#)].
- [61] T. Gehrmann, M. Jaquier, E. W. N. Glover, and A. Koukoutsakis, *Two-Loop QCD Corrections to the Helicity Amplitudes for  $H \rightarrow 3$  partons*, *JHEP* **02** (2012) 056, [[1112.3554](#)].
- [62] A. V. Kotikov, *Differential equations method: New technique for massive Feynman diagrams calculation*, *Phys. Lett.* **B254** (1991) 158–164.
- [63] E. Remiddi, *Differential equations for Feynman graph amplitudes*, *Nuovo Cim.* **A110** (1997) 1435–1452, [[hep-th/9711188](#)].
- [64] T. Gehrmann and E. Remiddi, *Analytic continuation of massless two loop four point functions*, *Nucl. Phys. B* **640** (2002) 379–411, [[hep-ph/0207020](#)].
- [65] J. Klappert, F. Lange, P. Maierhöfer, and J. Usovitsch, *Integral reduction with Kira 2.0 and finite field methods*, *Comput. Phys. Commun.* **266** (2021) 108024, [[2008.06494](#)].
- [66] A. V. Smirnov, *Algorithm FIRE – Feynman Integral REduction*, *JHEP* **10** (2008) 107, [[0807.3243](#)].

- [67] A. V. Smirnov and V. A. Smirnov, *FIRE4, LiteRed and accompanying tools to solve integration by parts relations*, *Comput. Phys. Commun.* **184** (2013) 2820–2827, [[1302.5885](#)].
- [68] A. V. Smirnov, *FIRE5: a C++ implementation of Feynman Integral REDuction*, *Comput. Phys. Commun.* **189** (2015) 182–191, [[1408.2372](#)].
- [69] A. V. Smirnov and F. S. Chuharev, *FIRE6: Feynman Integral REDuction with Modular Arithmetic*, *Comput. Phys. Commun.* **247** (2020) 106877, [[1901.07808](#)].
- [70] R. N. Lee, *Presenting LiteRed: a tool for the Loop InTEgrals REDuction*, [1212.2685](#).
- [71] R. N. Lee, *LiteRed 1.4: a powerful tool for reduction of multiloop integrals*, *J. Phys. Conf. Ser.* **523** (2014) 012059, [[1310.1145](#)].
- [72] T. Gehrmann and E. Remiddi, *Differential equations for two loop four point functions*, *Nucl. Phys.* **B580** (2000) 485–518, [[hep-ph/9912329](#)].
- [73] J. M. Henn, *Multiloop integrals in dimensional regularization made simple*, *Phys. Rev. Lett.* **110** (2013) 251601, [[1304.1806](#)].
- [74] J. M. Henn, *Lectures on differential equations for Feynman integrals*, *J. Phys. A* **48** (2015) 153001, [[1412.2296](#)].
- [75] M. Argeri, S. Di Vita, P. Mastrolia, E. Mirabella, J. Schlenk, U. Schubert, and L. Tancredi, *Magnus and Dyson Series for Master Integrals*, *JHEP* **03** (2014) 082, [[1401.2979](#)].
- [76] R. N. Lee, *Reducing differential equations for multiloop master integrals*, *JHEP* **04** (2015) 108, [[1411.0911](#)].
- [77] R. N. Lee, *Libra: a package for transformation of differential systems for multiloop integrals*, [2012.00279](#).
- [78] O. Gituliar and V. Magerya, *Fuchsia: a tool for reducing differential equations for Feynman master integrals to epsilon form*, *Comput. Phys. Commun.* **219** (2017) 329–338, [[1701.04269](#)].
- [79] M. Prausa, *epsilon: A tool to find a canonical basis of master integrals*, *Comput. Phys. Commun.* **219** (2017) 361–376, [[1701.00725](#)].
- [80] C. Dlapa, J. Henn, and K. Yan, *Deriving canonical differential equations for Feynman integrals from a single uniform weight integral*, *JHEP* **05** (2020) 025, [[2002.02340](#)].
- [81] T. Gehrmann, A. von Manteuffel, L. Tancredi, and E. Weihs, *The two-loop master integrals for  $q\bar{q} \rightarrow VV$* , *JHEP* **06** (2014) 032, [[1404.4853](#)].
- [82] M. Becchetti and R. Bonciani, *Two-Loop Master Integrals for the Planar QCD Massive Corrections to Di-photon and Di-jet Hadro-production*, *JHEP* **01** (2018) 048, [[1712.02537](#)].
- [83] K.-T. Chen, *Iterated path integrals*, *Bull. Amer. Math. Soc.* **83** (09, 1977) 831–879.
- [84] A. B. Goncharov, *Multiple polylogarithms, cyclotomy and modular complexes*, *Math. Res. Lett.* **5** (1998) 497–516, [[1105.2076](#)].
- [85] A. B. Goncharov, *Multiple polylogarithms and mixed Tate motives*, [math/0103059](#).
- [86] F. Brown and C. Duhr, *A double integral of dlog forms which is not polylogarithmic*, **6**, 2020. [2006.09413](#).

- [87] A. B. Goncharov, M. Spradlin, C. Vergu, and A. Volovich, *Classical Polylogarithms for Amplitudes and Wilson Loops*, *Phys. Rev. Lett.* **105** (2010) 151605, [[1006.5703](#)].
- [88] C. Duhr, H. Gangl, and J. R. Rhodes, *From polygons and symbols to polylogarithmic functions*, *JHEP* **10** (2012) 075, [[1110.0458](#)].
- [89] C. Duhr and L. Tancredi, *Algorithms and tools for iterated Eisenstein integrals*, *JHEP* **02** (2020) 105, [[1912.00077](#)].
- [90] S. Abreu, M. Becchetti, C. Duhr, and R. Marzucca, *Three-loop contributions to the  $\rho$  parameter and iterated integrals of modular forms*, *JHEP* **02** (2020) 050, [[1912.02747](#)].
- [91] M. Walden and S. Weinzierl, *Numerical evaluation of iterated integrals related to elliptic Feynman integrals*, [2010.05271](#).
- [92] S. Abreu, H. Ita, F. Moriello, B. Page, W. Tschernow, and M. Zeng, *Two-Loop Integrals for Planar Five-Point One-Mass Processes*, *JHEP* **11** (2020) 117, [[2005.04195](#)].
- [93] B. Jantzen, A. V. Smirnov, and V. A. Smirnov, *Expansion by regions: revealing potential and Glauber regions automatically*, *Eur. Phys. J.* **C72** (2012) 2139, [[1206.0546](#)].
- [94] J. Alwall, R. Frederix, S. Frixione, V. Hirschi, F. Maltoni, O. Mattelaer, H. S. Shao, T. Stelzer, P. Torrielli, and M. Zaro, *The automated computation of tree-level and next-to-leading order differential cross sections, and their matching to parton shower simulations*, *JHEP* **07** (2014) 079, [[1405.0301](#)].
- [95] C. Degrande, C. Duhr, B. Fuks, D. Grellscheid, O. Mattelaer, and T. Reiter, *UFO - The Universal FeynRules Output*, *Comput. Phys. Commun.* **183** (2012) 1201–1214, [[1108.2040](#)].
- [96] P. de Aquino, W. Link, F. Maltoni, O. Mattelaer, and T. Stelzer, *ALOHA: Automatic Libraries Of Helicity Amplitudes for Feynman Diagram Computations*, *Comput. Phys. Commun.* **183** (2012) 2254–2263, [[1108.2041](#)].
- [97] M. Bonetti, K. Melnikov, and L. Tancredi, *Three-loop mixed QCD-electroweak corrections to Higgs boson gluon fusion*, *Phys. Rev. D* **97** (2018), no. 3 034004, [[1711.11113](#)].